Spectroscopy of i'-Dropout Galaxies with an NB921-Band Depression in the Subaru Deep Field

T. Nagao [1,2], N. Kashikawa [2], M. A. Malkan [3], T. Murayama [4], Y. Taniguchi [4], K. Shimasaku [5], K. Motohara [6], M. Ajiki [4], Y. Shioya [4], K. Ohta [7], S. Okamura [5,8], and M. Iye [2]

ABSTRACT

We report new spectroscopy of two star-forming galaxies with strong Lyα emission at $z = 6.03$ and $z = 6.04$ in the Subaru Deep Field. These two objects are originally selected as i'-dropouts ($i' - z' > 1.5$) showing an interesting photometric property, the "NB921 depression". The $NB921$-band (centered at 9196Å) magnitude is significantly depressed with respect to the z'-band magnitude. The optical spectra of these two objects exhibit asymmetric emission-lines at $\lambda_{\rm obs} \sim 8540$Å and ~ 8560Å, suggesting that these objects are Lyα emitters at $z \sim 6$. The rest-frame equivalent widths of the Lyα emission of the two objects are 94Å and 236Å; the latter one is the Lyα emitter with the largest Lyα equivalent width at $z \gtrsim 6$ ever spectroscopically confirmed. The spectroscopically measured Lyα fluxes of these two objects are consistent with the interpretation that the NB921 depression is caused by the contribution of the strong Lyα emission to the z'-band flux. Most of the NB921-depressed i'-dropout objects are

[1]INAF – Osservatorio Astrofisico di Arcetri, Largo E. Fermi 5, 50125 Firenze, Italy; tohru@arcetri.astro.it

[2]National Astronomical Observatory of Japan, 2-21-1 Osawa, Mitaka, Tokyo 181-8588, Japan

[3]Department of Astronomy, University of California at Los Angeles, P. O. Box 951547, Los Angeles, CA 90095-1547

[4]Astronomical Institute, Graduate School of Science, Tohoku University, Aramaki, Aoba, Sendai 980-8578, Japan

[5]Department of Astronomy, Graduate School of Science, University of Tokyo, 7-3-1 Hongo, Bunkyo, Tokyo 113-0033, Japan

[6]Institute of Astronomy, Graduate School of Science, University of Tokyo, 2-21-1 Osawa, Mitaka, Tokyo 181-0015, Japan

[7]Department of Astronomy, Graduate School of Science, Kyoto University, Kitashirakawa, Sakyo, Kyoto 606-8502, Japan

[8]Research Center for the Early Universe, Graduate School of Science, University of Tokyo, Tokyo 113-0033, Japan

thought to be strong Lyα emitters at $6.0 \lesssim z \lesssim 6.5$; Galactic L and T dwarfs and NB921-dropout galaxies at $z > 6.6$ do not dominate the NB921-depressed i'-dropout sample. Thus the NB921-depression method is very useful for finding high-z Lyα emitters with a large Lyα equivalent width over a large redshift range, $6.0 \lesssim z \lesssim 6.5$. Although the broadband-selected sample at $z \sim 3$ contains only a small fraction of objects with a Lyα equivalent width larger than 100Å, the i'-dropout sample of the Subaru Deep Field contains a much larger fraction of such strong Lyα emitters. This may imply a strong evolution of the Lyα equivalent width from $z \gtrsim 6$ to $z \sim 3$.

Subject headings: early universe — galaxies: evolution — galaxies: formation — galaxies: individual (SDF J132426.5.0+271600 and SDF J132442.5+272423) — galaxies: starburst

1. INTRODUCTION

Observational studies of galaxy evolution generally rely on the investigation of statistical properties such as luminosity functions, correlation functions, distribution functions of mass and emission-line equivalent widths, as functions of redshift from $z \sim 0$ to the highest redshift, i.e., $z > 6$. This is one of the reasons why we should explore the highest-z universe and construct a highest-z galaxy sample. Recently, two alternative methods are often used to find high-z galaxies. One is to search for objects with a Lyman-break feature due to intergalactic absorption seen as a strong photometric discontinuity in the rest-frame UV stellar continuum spectrum (e.g., Steidel et al. 1996a, 1996b; Madau et al. 1996; Lowenthal et al. 1997). The other is to search for objects with a strong Lyα emission caused by massive stars using narrow passband filters (see for a review, Taniguchi et al. 2003). The high-z galaxies found in such ways are called "Lyman-break galaxies (LBGs)" and "Lyα emitters (LAEs)", respectively. These high-z galaxy surveys are now bringing us a sample of galaxies at $z > 6$ or the end of "the cosmic dark age" (e.g., Miralda-Escudé 2003; Djorgovski 2004). Recent narrow-band surveys pick up LAEs at $z \sim 6.6$ through an atmospheric window at ~ 9200Å (e.g., Hu et al. 2002; Kodaira et al. 2003; Rhoads et al. 2004; Taniguchi et al. 2005), and recent broad-band surveys pick up "i'-dropout galaxies" as candidates of galaxies at $z \sim 6$, which are characterized by a very red $i' - z'$ color due to a Lyman-break spectral feature (e.g., Stanway et al. 2003; Bouwens et al. 2003, 2004; Dickinson et al. 2004; Bunker et al. 2004). In order to investigate the nature of such high-z galaxy populations, follow-up spectroscopy is crucially important.

Recently, Nagao et al. (2004) reported the discovery of an interesting object among

48 i'-dropout galaxies detected in the Subaru Deep Field (SDF[1]; Kashikawa et al. 2004). The spectrum of this object, SDF J132440.6+273607, which has been obtained during the SDF follow-up spectroscopy campaign (see Taniguchi et al. 2005 for details), shows a very strong Lyα emission at 8909Å, i.e., $z = 6.33$, whose rest-frame equivalent width is as large as $EW_0 = 130$Å. However, this object does not show strong UV stellar continuum that is expected for i'-dropout galaxies. Thus the flux detected in the z' image is largely ($\sim$40%) attributed to the Lyα emission, giving a very red $i' - z'$ color. This discovery is important because only $\sim 1\%$ of broad-band selected LBGs at $z \sim 3$ show strong Lyα emission with $EW_0(\mathrm{Ly}\alpha) > 100$Å (Shapley et al. 2003). The finding of SDF J132440.6+273607 among such a small sample of i'-dropout galaxies may suggest that an i'-dropout sample contains strong LAEs much more frequently than a LBG sample at a redshift of $\sim$3.

To study this issue further, we focus on the 48 i'-dropout objects found in SDF. This is because we have not only deep i' and z' images but also a narrow-band image of NB921 [$(\lambda_{\mathrm{c}}, \Delta\lambda_{\mathrm{FWHM}}) = (9196$Å, 132Å); the transmission curves of these filters are shown in Figure 1]. This enables us to obtain information about the SED of the i'-dropout galaxies. As for SDF J132440.6+273607, due to the strong Lyα emission in the z' band (but out of the NB921 band), a significant "NB921 depression" is seen; i.e., $z' - NB921 = -0.54$. Interestingly, among the 48 i'-dropout objects in SDF, there are seven other objects with a NB921 depression with significance larger than 2σ of the sky noise (note that the significance level of NB921 depression for SDF J132440.6+273607 is slightly below 2σ). If all of these 7 objects are really similar objects (i.e., high-z galaxies with very large $EW_0(\mathrm{Ly}\alpha)$), SDF J132440.6+273607 would not be exceptional in the i'-dropout population. This might suggest a strong redshift evolution of the $EW_0(\mathrm{Ly}\alpha)$ distribution from $z \sim 6$ to $z \sim 3$ although it should be kept in mind that $z \sim 3$ LBGs and $z \sim 6$ i'-dropout galaxies are not selected by the same criteria.

In this paper, we report the results of our new spectroscopy of two i'-dropout objects with a significant NB921 depression. Throughout this paper, we adopt a cosmology with $(\Omega_{\mathrm{tot}}, \Omega_{\mathrm{M}}, \Omega_{\Lambda}) = (1.0, 0.3, 0.7)$ and $H_0 = 70$ km s^{-1} Mpc^{-1}. We use the AB photometric system for optical magnitudes.

---

[1]The SDF project consists of multi-color deep imaging observations by Suprime-Cam (Miyazaki et al. 2002) and spectroscopic observations by FOCAS (Kashikawa et al. 2002), boarded on the Subaru Telescope (Kaifu et al. 2000; Iye et al. 2004). SDF is centered on ($13^h24^m38\overset{s}{.}9$, $+27°29'25\overset{''}{.}9$) (J2000.0). See Kashikawa et al. (2004) and Taniguchi et al. (2005) for more details.

2. OBSERVATIONS

The SDF spectroscopic follow-up campaign has been carried out with DEIMOS (Faber et al. 2003) on the Keck II telescope, on 2 nights in April 2004. During this observing run, we obtained spectra of i'-dropout objects which were selected by the following four criteria; (1) $i' - z' > 1.5$, (2) $z' < 26.1$ (i.e., above 5σ), (3) $B > 28.5$ (below 3σ), and (4) $R_{\rm C} > 27.8$ (below 3σ). The adopted $i' - z'$ color criterion is the same as that adopted for i'-dropouts by Stanway et al. (2003). In this observing run, we observed two NB921-depressed objects, SDF J132426.5+271600 and SDF J132442.5+272423 among seven NB921-depressed i'-dropout objects in the SDF. Here the objects that satisfy the fifth criterion are classified as NB921-depressed i'-dropout objects; (5) $z' - NB921$ showing a depression whose significance level is larger than 2σ of the sky noise. In Figure 2, the photometric properties of the 48 i'-dropout objects in SDF are shown on a $z' - NB921$ versus z' color-magnitude diagram and a $z' - NB921$ versus $i' - z'$ color-color diagram. The photometric properties of the targeted two objects are given in Table 1. See Kashikawa et al. (2004) for details of the SDF imaging observations.

The spectra of SDF J132426.5+271600 and SDF J132442.5+272423 were obtained on 23 April 2004 (UT). The 830 lines/mm grating and the GG495 order-sorting filter were used. The resulting wavelength coverage was ~ 6000Å $- 9600$Å, with a dispersion of 0.47 Å/pixel. The adopted slit width was 1.0 arcsec, which gave a spectral resolution of $R \sim 3600$ at 8500Å, which is measured by the widths of atmospheric OH emission lines. The total integration time was 7929 sec for SDF J132426.5+271600 and 7058 sec for SDF J132442.5+272423. The weather was clear and photometric, and the typical seeing size was 0.7 – 1.0 arcsec during the observation. We also obtained spectra of a spectrophotometric standard star Feige 110 (Oke 1990) for the flux calibration. The obtained data were reduced by the DEEP2 DEIMOS data reduction software, the spec2d pipeline[2].

3. RESULTS

In Figure 3, the sky-subtracted optical spectra are plotted with a typical sky spectrum. Both objects show a single strong emission line, with peak wavelengths of 8540Å and 8560Å for SDF J132426.5+271600 and SDF J132442.5+272423, respectively. No continuum emission is detected for both objects. Both emission lines show a clear asymmetric profile; i.e., a sharp decline on the blue side and a prominent tail on the red side of the line. Spiky features

[2]The data reduction pipeline was developed at UC Berkeley with support from NSF grant AST-0071048.

redward of the emission line of SDF J132426.5+271600 seem to be the residuals of the sky emission. The redward tails extend to $\sim$ 8564Å and $\sim$ 8577Å for SDF J132426.5+271600 and SDF J132442.5+272423 respectively. To quantify the asymmetry of the lines, we measured the flux ratio between $f_{\rm red}$ and $f_{\rm blue}$, where $f_{\rm red}$ is the flux at wavelengths longer than the peak while $f_{\rm blue}$ is that at wavelengths shorter. The measured ratios are 2.5 ± 0.4 and 1.6 ± 0.2 for SDF J132426.5+271600 and SDF J132442.5+272423 respectively, which are significantly larger than unity, although the spiky noise redward of the emission line of SDF J132426.5+271600 would affect the ratio. This is consistent with the interpretation that the detected emission line is Lyα, not any other emission line (see Taniguchi et al. 2005). The observed line-shape asymmetry and the photometric properties strongly suggest that SDF J132426.5+271600 and SDF J132442.5+272423 are at $z = 6.03$ and $z = 6.04$, respectively. This interpretation is supported by the fact that no other emission lines are detected for both objects, because Hα, Hβ, or [OIII]λ5007 emitters at $z \sim 0.30$, $z \sim 0.76$, or $z \sim 0.71$ (which are possible candidates for line emitters at $\sim$ 8550Å) should show [OIII] at $\sim$ 6510Å, [OIII] at $\sim$ 8810Å or Hβ at $\sim$ 8310Å, respectively. The possibility that the observed objects are [OII] emitters at $z \sim 1.29$ is rejected by the obtained emission-line profiles, because the expected wavelength separation of the [OII] doublet for objects at $z = 1.29$ is $\Delta\lambda \sim 6.4$Å, which should be resolved by our wavelength resolution of $R \sim 3600$. Note that the wavelength separation of the emission-line peak and the spiky feature redward of the emission line of SDF J132426.5+271600 is $\sim$ 8Å, rather larger than the separation expected for the [OII] doublet from an object at $z = 1.29$. We also note that the $i' - z'$ color of foreground galaxies at $z < 1.3$ is expected to be bluer than 1.5 mag, even when the SED of passively evolved elliptical-type galaxies is assumed (e.g., Stanway et al. 2003). We thus conclude that the observed two objects are strong LAEs at $z = 6.03$ and $z = 6.04$.

Adopting these redshifts, the NVλ1240 emission would be expected at $\sim$ 8680Å if these two objects are AGNs at $z \sim 6$. However, no such emission-line features are seen in this wavelength for either object (Figure 3). The 3σ upper limit for the NVλ1240 emission is 9.5×10^{-18} ergs s^{-1} cm^{-2} and 9.3×10^{-18} ergs s^{-1} cm^{-2} for SDF J132426.5+271600 and SDF J132442.5+272423 respectively. However, we cannot reject the possibility that these two objects are AGNs only by these weak constraints on the NVλ1240 fluxes. Indeed it is known that some high-z narrow-line radio galaxies show very weak NVλ1240 emission compared with Lyα (e.g., De Breuck et al. 2000; Nagao et al. 2005a). In order to examine this issue further, follow-up spectroscopy in the near-infrared is required to see some high-ionization emission lines such as CIVλ1549 attributed to AGN. Despite this uncertainty, however, we regard these two observed objects as star forming galaxies but not AGNs in the following analysis and discussion.

The Lyα fluxes of SDF J132426.5+271600 and SDF J132442.5+272423 are $(3.6 \pm 0.3) \times$

10^{-17} ergs s^{-1} cm^{-2} and $(4.5\pm0.3)\times10^{-17}$ ergs s^{-1} cm^{-2}, respectively, giving Lyα luminosities of $(1.5 \pm 0.1) \times 10^{43}$ ergs s^{-1} and $(1.8 \pm 0.1) \times 10^{43}$ ergs s^{-1} (where the slit losses are not taken into account). The measured emission-line widths of SDF J132426.5+271600 and SDF J132442.5+272423 are 12.0Å and 6.8Å in full-width at half maximum (FWHM), corresponding to 410 km s^{-1} and 220 km s^{-1} where the instrumental broadening effect is quadratically corrected. The estimated line widths at zero intensity (FWZI) are 29.5Å and 22.0Å, corresponding to 1030 km s^{-1} and 770 km s^{-1}, respectively. The measured spectroscopic properties of the two observed objects are summarized in Table 2.

While the $NB921$-band flux is attributed only to the stellar UV continuum emission, the z'-band fluxes of the two observed objects apparently contain much Lyα flux. The estimated fractions of the z'-band flux contributed by Lyα are $\sim 25\%$ and $\sim 46\%$ for J132426.5+271600 and SDF J132442.5+272423, respectively. The UV continuum flux densities derived from the $NB921$ magnitudes are 5.5×10^{-20} ergs s^{-1} cm^{-2} Å^{-1} and 2.7×10^{-20} ergs s^{-1} cm^{-2} Å^{-1}, respectively. We then estimate the Lyα-subtracted z'-band magnitude, by subtracting the spectroscopically measured Lyα flux from the z'-band flux. Note that this procedure may result in an over-subtraction due to a short-wavelength cutoff of the z'-filter transmission. The estimated magnitudes are $z'_{\rm cor} = 25.7$ and $z'_{\rm cor} = 26.6$ for SDF J132426.5+271600 and SDF J132442.5+272423, respectively. These magnitudes are nearly the same as the $NB921$ magnitudes within the range of < 0.2 mag. This result suggests that the NB921 depression is caused mainly by the contribution of the Lyα flux into the z'-band flux.

For narrow-band selected high-z LAEs, it is sometimes difficult to estimate EW_0(Lyα) because the measurements of continuum flux on the low-S/N spectra are generally very hard. Indeed only upper-limits to the UV continuum flux density and resulting lower limits to EW_0(Lyα) have been obtained for such LAEs in most of the previous high-z (i.e., $z \gtrsim 6$) LAE studies (e.g., Kodaira et al. 2003; Kurk et al. 2004; Taniguchi et al. 2005). However, for SDF J132426.5+271600 and SDF J132442.5+272423, we can estimate EW(Lyα) rather straightforwardly by referring to the $NB921$-band flux to determine the continuum levels, if we assume a flat UV SED. The estimated values of $EW_{\rm obs}$(Lyα) are 660 Å and 1659 Å, giving EW_0(Lyα) = 94 Å and EW_0(Lyα) = 236 Å for SDF J132426.5+271600 and SDF J132442.5+272423, respectively. Note that if the detected emission lines were [OII]λ3727, the rest-frame equivalent widths would be 288Å and 724Å, respectively. These values are implausibly large for low-z [OII] emitters (e.g., Ajiki et al. 2005), which also supports our interpretation that the detected emission lines are Lyα. Here we mention that the derived EW_0(Lyα) for SDF J132442.5+272423 is the largest one among the spectroscopically identified galaxies ever known at $z \gtrsim 6$.

4. DISCUSSION

4.1. The Nature of $NB921$-Depressed i'-Dropout Objects

Although SDF J132426.5+271600 and SDF J132442.5+272423 turned out to be strong LAEs at $z \sim 6$, it does not necessarily mean that all of the NB921-depressed i'-dropout objects are similar strong LAEs. We point out that there are three possibilities for the NB921-depressed i'-dropout objects; Galactic very late-type stars, NB921-dropout galaxies at $z > 6.6$, and strong Lyα emitters at $6.0 \lesssim z \lesssim 6.5$. To understand the nature of the observed objects selected by the criterion "NB921-depressed i'-dropout", we discuss each possibility below.

4.1.1. Galactic Late-Type Stars

Objects selected by i'-dropout criterion are not necessarily high-z galaxies; sometimes Galactic late-type stars contaminate in i'-dropout samples (e.g., Stanway et al. 2004). The NB921 depression might be accompanied with such late-type stars owing to their strong and complex molecular absorption spectral features. Therefore it is worthwhile to examine whether such Galactic late-type stars can be selected as NB921-depressed i'-dropout objects before considering the possibility that they are really very high-z galaxies. In Figure 4, the photometric properties of the NB921-depressed i'-dropout objects are compared with those of Galactic stars on a $z' - NB921$ versus $i' - z'$ color-color diagram. Here we use Gunn & Stryker (1983) for photometric properties of Galactic M type and earlier, and Kirkpatrick (2003) for those of L and T dwarf stars. This figure shows that Galactic L and T dwarfs exhibit red $i' - z'$ color ($i' - z' > 1.5$) and thus are selected as i'-dropout objects, but none of them exhibit significant NB921 depression. The bluest $z' - NB921$ color of the L and T dwarfs is $z' - NB921 \sim +0.1$, which is too red to reproduce the observed NB921 depressions seen in our i'-dropout subsample. Although the possibility that Galactic stars are included in the NB921-depressed i'-dropout sample cannot be completely discarded when taking the photometric uncertainties into account, Figure 5 suggests that late-type Galactic stars are not a dominant population in the NB921-depressed i'-dropout sample.

4.1.2. NB921-Dropout Galaxies at $z > 6.6$

We now consider the second possibility that the NB921-depressed i'-dropout galaxies are "NB921-dropout galaxies", i.e., galaxies at $z > 6.6$ and thus the Lyman-break feature

drops at a longer wavelength than the NB921 band. See Shioya et al. (2005) for general discussion on NB921-dropout galaxies. To see the photometric properties of the NB921-dropout galaxies quantitatively, theoretically calculated $z' - NB921$ color is plotted as a function of redshift in Figure 5. The adopted stellar spectrum is created by the stellar population model GALAXEV (Bruzual & Charlot 2003) assuming a stellar metallicity of $Z = 0.02$, a Salpeter initial mass function ($0.1 \leq M/M_{\odot} \leq 100$), and an exponentially decaying star-formation history with the timescale of $\tau = 1$ Gyr and the age of 1 Gyr. Although no dust reddening is taken into account for models shown in Figure 6, a moderate amount of the reddening does not affect the $z' - NB921$ color significantly; a dust reddening of $E(B-V) = 0.3$ mag changes the $z' - NB921$ color less than ± 0.2 mag. Models with $EW_0(\mathrm{Ly}\alpha) = 0$, 65, 130, and 260 Å are plotted in the figure. As shown in Figure 5, significant NB921 depressions can be caused at the redshift range of $6.7 \lesssim z \lesssim 7.2$ due to the combination of the absorption of the $NB921$ flux by the intergalactic matter and the contribution of the Lyα contribution into the z'-band flux. However, the z'-band flux of galaxies at $z > 6.6$ decreases so significantly that the detection of such NB921-dropout galaxies is very difficult. In Figure 6, the expected z' magnitude of galaxies with an absolute magnitude of $M_{1500} = -20.0$ is shown as a function of redshift. The adopted SEDs are the same as those in Figure 6. It is clearly shown that the z'-band flux is decreasing at $z > 6.6$, especially for the galaxies with no or weak Lyα emission. Shioya et al. (2005) predicted the expected number of NB921-dropout galaxies in the FOV of the SDF. They reported that the expected number of NB921-dropout galaxies with $z' < 26.1$ mag is ≈0.03 if a starburst SED without Lyα is assumed and ≈1.2 if $EW_0(\mathrm{Ly}\alpha) = 65$ Å is assumed (here a UV luminosity function at $z \sim 6$ reported by Bouwens et al. 2004 is adopted). This suggests that the NB921-dropout galaxies (i.e., galaxies at $z > 6.6$) are at most a minor population in the NB921-depressed i'-dropout sample.

4.1.3. Strong LAEs at $6.0 \lesssim z \lesssim 6.5$

For the two LAEs presented in this paper and another LAE reported by Nagao et al. (2004), the NB921 depression of the NB921-depressed i'-dropout objects can be attributed to the large Lyα contribution in the z'-band flux if the strong LAE is in proper redshift range. As shown in Figure 5, the $z' - NB921$ color is not affected by Lyα at $z \lesssim 5.8$ because Lyα is out of the z' band. At $6.0 \lesssim z \lesssim 6.5$, the NB921 depression is caused by a contribution of strong Lyα emission into the z'-band. Indeed we carried out spectroscopy of the three such objects in the SDF (two in this paper and one in Nagao et al. 2004; see Figure 2) and all of the three objects now turn out to be strong LAEs with $EW_0(\mathrm{Ly}\alpha) \gtrsim 100$Å at the redshift range of $6.0 \lesssim z \lesssim 6.5$. Since Galactic late-type dwarfs and NB921-dropout galaxies

at $z > 6.6$ are thought not to be a dominant populations in the NB921-depressed i'-dropout objects, most of the NB921-depressed i'-dropout galaxies seem to be strong LAEs, and their NB921 depression seems to be caused by the large Lyα contribution into the z'-band flux.

4.2. NB921-Depression Method to Search for Strong LAEs

We have shown that the NB921-depression is a powerful search method for strong LAEs. First, by this method one can search for high-z LAEs with a large EW_0(Lyα) in a larger redshift range, $6.0 \lesssim z \lesssim 6.5$, than the traditional NB921-excess method ($6.5 \lesssim z \lesssim 6.6$). Although Ajiki et al. (2004) proposed a method of LAE surveys using an intermediate-band filter in order to sweep larger volumes than those using the usual narrow-band filters (see also Fujita et al. 2003), the NB921-depression method can sweep a much larger volume for strong LAEs. And second, this method picks up LAEs with a very large EW_0(Lyα) selectively. The LAEs with a large EW_0(Lyα) are highly interesting because a very young stellar population or a top-heavy initial-mass function would be expected for LAEs with EW_0(Lyα) > 100Å (e.g., Leitherer et al. 1999; Malhotra & Rhoads 2002). And more interestingly, a population III stellar cluster is also expected to show very large EW_0(Lyα) because it radiates much more hydrogen-ionizing photons per unit mass than population I/II stellar clusters (e.g., Schaerer 2002, 2003; Venkatesan, Tumlinson, & Shull 2003; Scannapieco, Schneider, & Ferrara 2003). To pursue these interesting high-z populations, the NB921-depression method is a highly efficient strategy (see also Nagao et al. 2005b) and thus the application of this method to other deep fields will be an excellent way to investigate high-z populations further.

Our interest in LAEs with a large EW_0(Lyα) naturally leads to the following question: does the frequency distribution of EW_0(Lyα) evolve on a cosmological timescale? At $z \sim 3$, $\approx$1% of LBGs (i.e., broadband-selected objects) show EW_0(Lyα) > 100Å (Sharpley et al. 2003). On the contrary, at $z \gtrsim 6$, at least 3 objects among 48 i'-dropout objects in SDF show EW_0(Lyα) > 100Å. Note that we are now focusing on broadband-selected objects; narrow-band selected objects tend to show much larger EW_0(Lyα) (e.g., Malhotra & Rhoads 2002; Dawson et al. 2004). Since other 5 NB921-depressed i'-dropout galaxies would also possibly possess EW_0(Lyα) > 100Å as discussed above, our results suggest that the frequency distribution of EW_0(Lyα) evolves significantly from $z \gtrsim 6$ to $z \sim 3$, which may imply the evolution of some properties of stellar populations such as the mean stellar age or the initial mass function (see, e.g., Kudritzki et al. 2000; Malhotra & Rhoads 2002). Note that some difference in the EW_0(Lyα) frequency distribution is caused by a selection effect, because LBGs at $z \sim 3$ are selected by two colors while i'-dropout galaxies at $z \gtrsim 6$ are selected by a $i' - z'$ color alone. Our criterion for i' dropouts, $i' - z' > 1.5$, is so strict that we might

pick up objects with a large $EW_0(\mathrm{Ly}\alpha)$ selectively. This issue should be examined more quantitatively by future complete spectroscopic surveys of i'-dropout galaxies. We should also be aware that we see somewhat different ranges of the luminosity functions for the $z \sim 3$ sample and the $z \gtrsim 6$ sample discussed here. While the spectroscopic survey for the $z \sim 3$ LBG sample by Sharpley et al. (2003) reaches down to $R_{\rm AB} \sim 25.5$ mag which corresponds to $L_{\rm lim} \sim L_*(z = 3) + 1.0$ (see Steidel et al. 1999), the SDF i'-dropout sample consists of galaxies with $z' > 25.9$ mag which corresponds to $L_{\rm lim} \sim L_*(z = 6) + 0.5$ if adopting the UV luminosity function at $z \sim 6$ reported by Bouwens et al. (2004). While the above discussion on the evolution of the $EW_0(\mathrm{Ly}\alpha)$ frequency distribution would not be affected if emission-line equivalent widths are independent of luminosity of galaxies as suggested by, e.g., van Dokkum et al. (2004), other observations imply that the emission-line equivalent widths may depend on the luminosity of galaxies (e.g., Ando et al. 2004). We do not discuss this issue further because this topic is beyond the scope of this paper.

4.3. Star-Formation Rates of $NB921$-Depressed i'-Dropout Galaxies

We now consider the star-formation rates (SFRs) of the NB921-depressed i'-dropout galaxies. The SFRs of the two NB921-depressed i'-dropout galaxies are obtained by adopting the following relation; $SFR(\mathrm{Ly}\alpha) = 9.1 \times 10^{-43}\ L(\mathrm{Ly}\alpha)\ M_\odot\ \mathrm{yr}^{-1}$ where $L(\mathrm{Ly}\alpha)$ is in units of ergs s^{-1} (Kennicutt1998; Brocklehurst 1971). Then $SFR(\mathrm{Ly}\alpha) = 13.4\ M_\odot\ \mathrm{yr}^{-1}$ and $SFR(\mathrm{Ly}\alpha) = 16.6\ M_\odot\ \mathrm{yr}^{-1}$ for SDF J132426.5+271600 and SDF J132442.5+272423, respectively. These SFRs are lower limits because no corrections are made for possible absorption effects on the Lyα emission. We can also estimate the SFRs from the luminosity of the UV stellar continuum by adopting the following relation; $SFR(\mathrm{UV}) = 1.4 \times 10^{-28} L_\nu M_\odot \mathrm{yr}^{-1}$ (Kennicutt 1998). By using the UV continuum flux densities measured from the $NB921$ magnitudes, we obtain $SFR(\mathrm{UV}) = 9.9\ M_\odot\ \mathrm{yr}^{-1}$ and $SFR(\mathrm{UV}) = 4.8\ M_\odot\ \mathrm{yr}^{-1}$ for SDF J132426.5+271600 and SDF J132442.5+272423, respectively. Here the Salpeter initial mass function (0.1–100 $M_\odot$) and the flat UV SED are assumed to derive $SFR(\mathrm{Ly}\alpha)$ and $SFR(\mathrm{UV})$ (see Kennicutt 1998).

The ratios of SFRs estimated by the two methods, $SFR(\mathrm{Ly}\alpha)/SFR(\mathrm{UV})$, are significantly higher than unity in both of the two observed objects, which is similar to the other NB921-depressed i'-dropout galaxy reported by Nagao et al. (2004). This result is interesting because high-z LAEs with smaller $EW_0(\mathrm{Ly}\alpha)$ tend to show the opposite trend (i.e., $SFR(\mathrm{Ly}\alpha)/SFR(\mathrm{UV}) < 1$; e.g., Hu et al. 2002; Ajiki et al. 2003; Taniguchi et al. 2005), possibly due to resonance scattering effects on the Lyα emission. As mentioned by Nagao et al. (2004), this systematic difference in the ratio of $SFR(\mathrm{Ly}\alpha)/SFR(\mathrm{UV})$ between LAEs

with small $EW_0(\mathrm{Ly}\alpha)$ and large $EW_0(\mathrm{Ly}\alpha)$ may be due to a different stellar population because large $EW_0(\mathrm{Ly}\alpha)$ (> 100Å) is difficult to reproduce by continuous star formation with a normal initial mass function, which is assumed when we derive the SFRs. This trend is consistent with the description of Schaerer (2000) in which $SFR(\mathrm{UV})$ is underestimated for star-forming galaxies with an age of $< 10^8$ yr (see also, e.g., Leitherer et al. 1999; Malhotra & Rhoads 2002).

5. SUMMARY

Based on DEIMOS follow-up spectroscopy of objects imaged in the SDF, we identified two NB921-depressed i'-dropout objects to be strong LAEs at $z \sim 6$. Taking both this finding and theoretical considerations into account, we conclude that most of the NB921-depressed i'-dropout objects in the SDF are strong LAEs at $6.0 \lesssim z \lesssim 6.5$. The presence of a large fraction of LAEs with a large $EW_0(\mathrm{Ly}\alpha)$ may imply the evolution of $EW_0(\mathrm{Ly}\alpha)$ at high redshift. This has implications for the cosmological evolution of stellar populations, and the existence of a population III.

The SDF project is one of the investigations promoted by the Subaru Telescope, which is operated by the National Astronomical Observatory of Japan. We thank the staffs of the Subaru Telescope and of the W. M. Keck Observatory. We also thank M. Doi for his contribution to the data acquisition. TN and MA are JSPS fellows. This research is partly supported by the Japan Society for the Promotion of Science (JSPS) through Grant-in-Aid 15340059 and 16740118, and by the Ministry of Education, Culture, Sports, Science and Technology (10044052 and 10304013). TN and MA are JSPS fellows.

REFERENCES

Ajiki, M., et al. 2003, AJ, 126, 2091

Ajiki, M., et al. 2004, PASJ, 56, 597

Ajiki, M., et al. 2005, PASJ, submitted

Ando, M., Ohta, K., Iwata, I., Watanabe, C., Tamura, N., Akiyama, M., & Aoki, K. 2004, ApJ, 610, 635

Bouwens, R. J., et al. 2003, ApJ, 595, 589

Bouwens, R. J., et al. 2004, ApJ, 606, L25

Brocklehurst, M. 1971, MNRAS, 153, 471

Bruzual, G., & Charlot, S. 2003, MNRAS, 344, 1000

Bunker, A. J., Stanway, E., Ellis, R. S., & McMahon, R. G. 2004, MNRAS, 355, 374

Dawson, S., et al. 2004, ApJ, 617, 707

De Breuck, C., Röttgering, H., Miley, G., van Breugel, W., & Best, P. 2000, A&A, 362, 519

Dickinson, M., et al. 2004, ApJ, 600, L99

Djorgovski, S. G. 2004, Nature, 427, 790

Faber, S. M., et al. 2003, SPIE, 4841, 1657

Fujita, S. S., et al. 2003, AJ, 125, 13

Giavalisco, M., et al. 2004, ApJ, 600, L103

Gunn, J. E., & Stryker, L. L. 1983, ApJS, 52, 121

Hu, E. M., Cowie, L. L., McMahon, R. G., Capak, P., Iwamuro, F., Kneib, J. -P., Maihara, T., & Motohara, K. 2002, ApJ, 568, L75

Iye, M., et al. 2004, PASJ, 56, 381

Kaifu, N., et al. 2000, PASJ, 52, 1

Kashikawa, N., et al. 2002, PASJ, 54, 819

Kashikawa, N., et al. 2004, PASJ, 56, 1011

Kennicutt, R. C., Jr. 1998, ARA&A, 36, 189

Kirkpatrick, J. D. 2003, IAUS, 211, 189

Kodaira, K., et al. 2003, PASJ, 55, L17

Kudritzki, R. -P., et al. 2000, ApJ, 536, 19

Kurk, J. D., Cimatti, A., di Serego Alighieri, S., Vernet, J., Daddi, E., Ferrara, A., & Ciardi, B. 2004, A&A, 422, L13

Leitherer, C., et al. 1999, ApJS, 123, 3

Lowenthal, J. D., et al. 1997, ApJ, 481, 673

Madau, P., Ferguson, H. C., Dickinson, M. E., Giavalisco, M., Steidel, C. C., & Fruchter, A. 1996, MNRAS, 283, 1388

Malhotra, S., & Rhoads, J. E. 2002, ApJ, 565, L71

Miralda-Escudé, J. 2003, Science, 300, 1904

Miyazaki, S., et al. 2002, PASJ, 54, 833

Nagao, T., et al. 2004, ApJ, 613, L9

Nagao, T., Maiolino, R., & Marconi, A. 2005a, in preparation

Nagao, T., Motohara, K., Maiolino, R., Marconi, A., Taniguchi, Y., Aoki, K., Ajiki, M., & Shioya, Y. 2005b, ApJ, submitted

Oke, J. B. 1990, AJ, 99, 1621

Rhoads, J. E., et al. 2004, ApJ, 611, 59

Scannapieco, E., Schneider, R., & Ferrara, A. 2003, ApJ, 589, 35

Schaerer, D. 2000, in Building the Galaxies: From the Primordial Universe to the Present, eds. F. Hammer, et al. (Gif-sur-Yvette: Editions Frontières), 389

Schaerer, D. 2002, A&A, 382, 28

Schaerer, D. 2003, A&A, 397, 527

Shapley, A. E., Steidel, C. C., Pettini, M., & Adelberger, K. L. 2003, ApJ, 588, 65

Shioya, Y., et al. 2005, PASJ, in press (astro-ph/0507270)

Stanway, E., Bunker, A. J., & McMahon, R. G. 2003, MNRAS, 342, 439

Stanway, E., Bunker, A. J., McMahon, R. G., Ellis, R. S., Treu, T., & McCarthy, P. J. 2004, ApJ, 607, 704

Steidel, C. C., Adelberger, K. L. , Giavalisco, M., Dickinson, M., & Pettini, M. 1999, ApJ, 519, 1

Steidel, C. C., Giavalisco, M., Dickinson, M., & Adelberger, K. L. 1996a, AJ, 112, 352

Steidel, C. C., Giavalisco, M., Pettini, M., Dickinson, M., & Adelberger, K. L. 1996b, ApJ, 462, L17

Taniguchi, Y., et al. 2005, PASJ, 57, 165

Taniguchi, Y., Shioya, Y., Ajiki, M., Fujita, S. S., Nagao, T., & Murayama, T. 2003, JKAS, 36, 123; Erratum, JKAS, 36, 283

van Dokkum, P. G., et al. 2004, ApJ, 611, 703

Venkatesan, A., Tumlinson, J., & Shull, J. M. 2003, ApJ, 584, 621

Table 1. Photometric Properties of the Target Objects

Object	Band	Magnitude[a] (mag)
SDF J132426.5+271600	B	> 28.5[b]
	$R_{\rm C}$	> 27.8[b]
	i'	27.43
	z'	25.36
	$NB921$	25.92
SDF J132442.5+272423	B	> 28.5[b]
	$R_{\rm C}$	> 27.8[b]
	i'	27.69
	z'	25.74
	$NB921$	26.71

[a]AB magnitude measured within a $2\farcs0$ diameter aperture.

[b]3σ upper-limit magnitudes.

Table 2. Spectroscopic Properties of the Target Objects

Object	Redshift	$F(\mathrm{Ly}\alpha)$ (10^{-17} ergs/s/cm^2)	$L(\mathrm{Ly}\alpha)$ (10^{43} ergs/s)	FWHM[a] (km/s)	FWZI[a] (km/s)	$f_{\mathrm{red}}/f_{\mathrm{blue}}$	$EW_0(\mathrm{Ly}\alpha)$ (Å)
SDF J132426.5+271600	6.03	3.6 ± 0.3	1.5 ± 0.1	410	1030	2.5 ± 0.4	94
SDF J132442.5+272423	6.04	4.5 ± 0.3	1.8 ± 0.1	220	770	1.6 ± 0.2	236

[a]Corrected for the instrumental broadening.

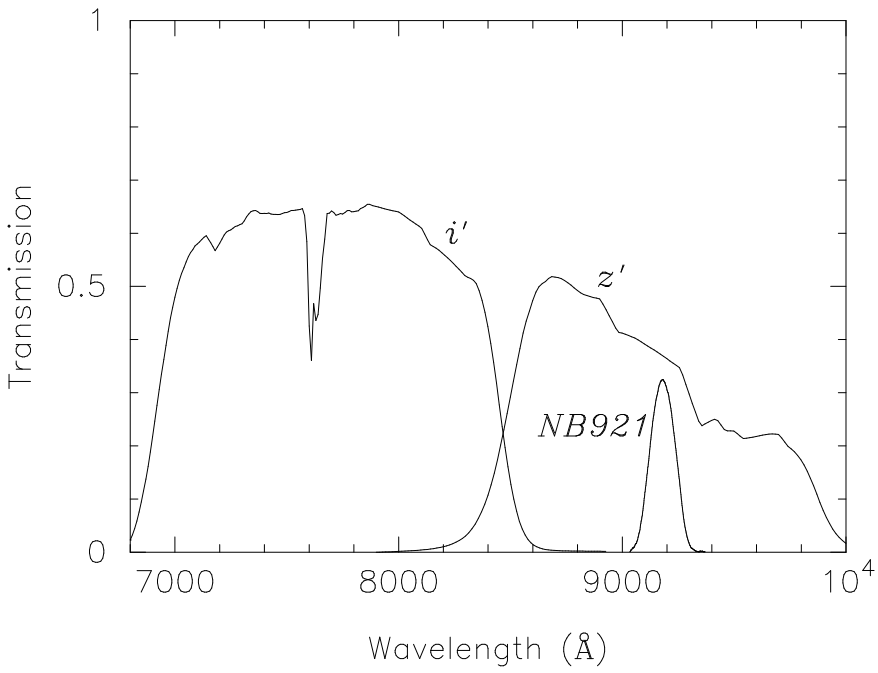

Fig. 1.— Transmission curves of the i', z' and $NB921$ filters installed in Suprime-Cam. The response curve of MIT CCD detectors on Suprime-Cam, the efficiency of the telescope optics including the mirror and the prime-focus corrector, and the atmospheric opacity ($\sec z = 1.2$) are taken into account.

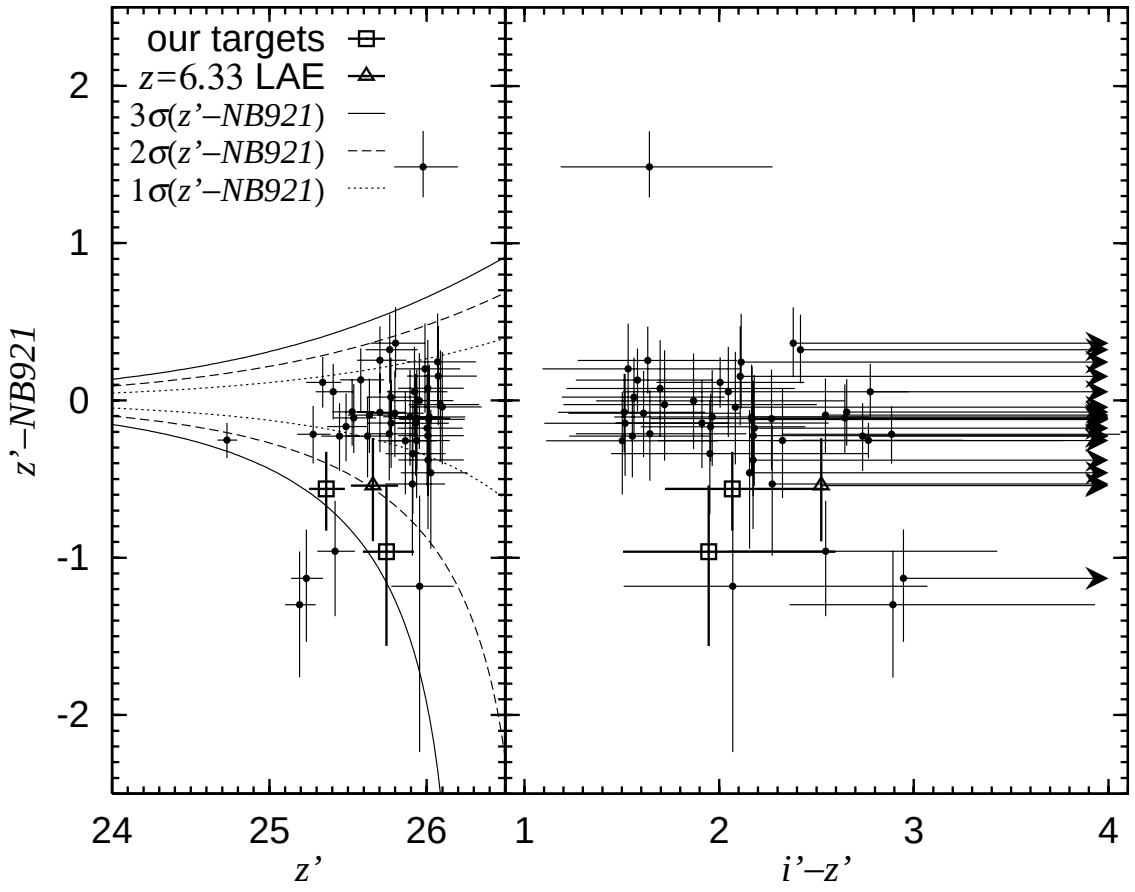

Fig. 2.— $z' - NB921$ versus z' color-magnitude diagram ($left$) and $z' - NB921$ versus $i' - z'$ color-color diagram ($right$). The 48 i'-dropout objects detected in the SDF are plotted. The two target objects among them (SDF J132426.5+271600 and SDF J132442.5+272423) are shown by open squares, and the objects discussed by Nagao et al. (2004) is shown by a open triangle. In the left panel, 1σ, 2σ, and 3σ uncertainties of the color of $z' - NB921$ are shown by the dotted, dashed, and solid lines, respectively.

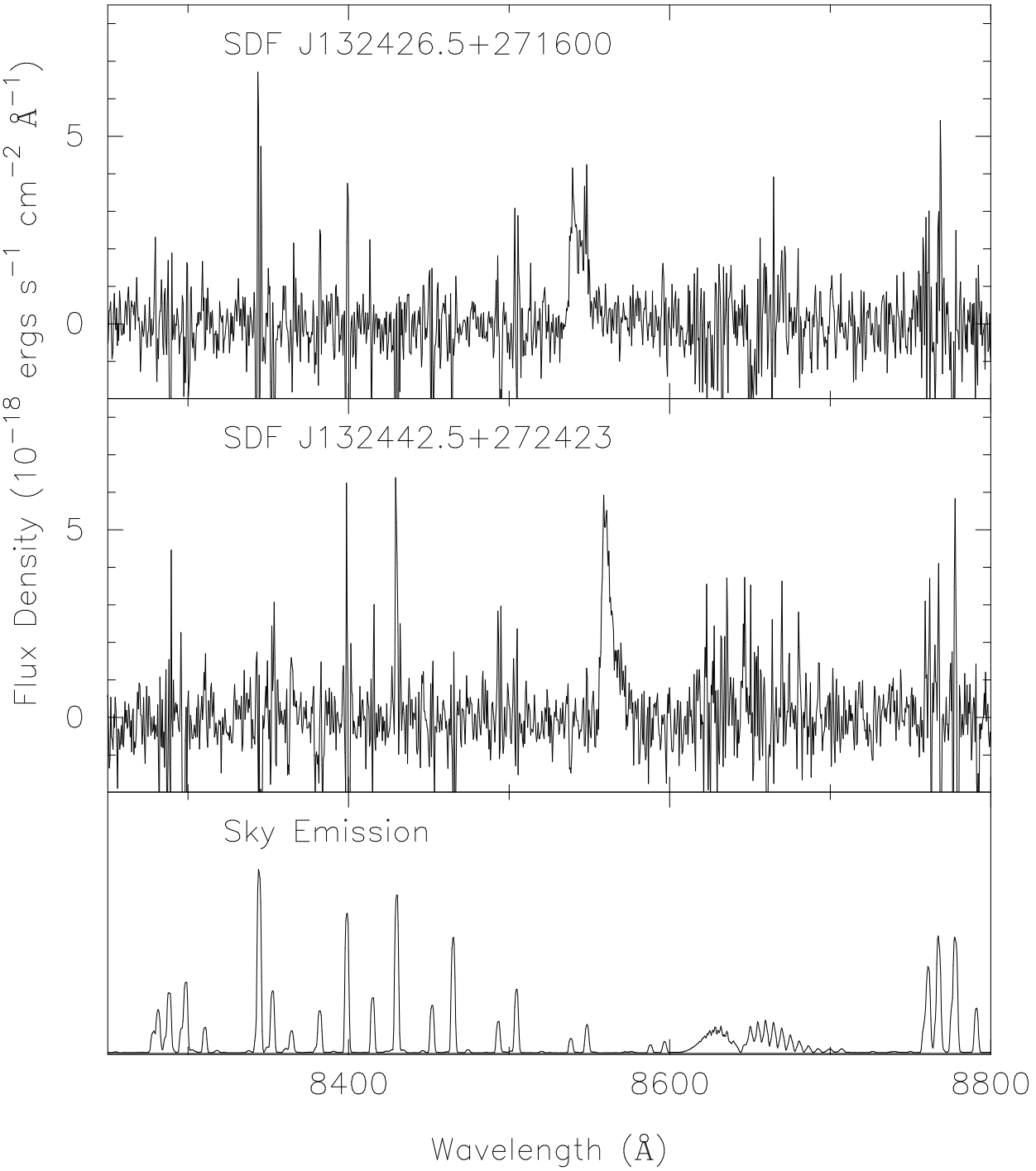

Fig. 3.— Optical spectra of SDF J132426.5+271600 (*upper*), SDF J132442.5+272423 (*middle*) and typical sky emission (*lower*).

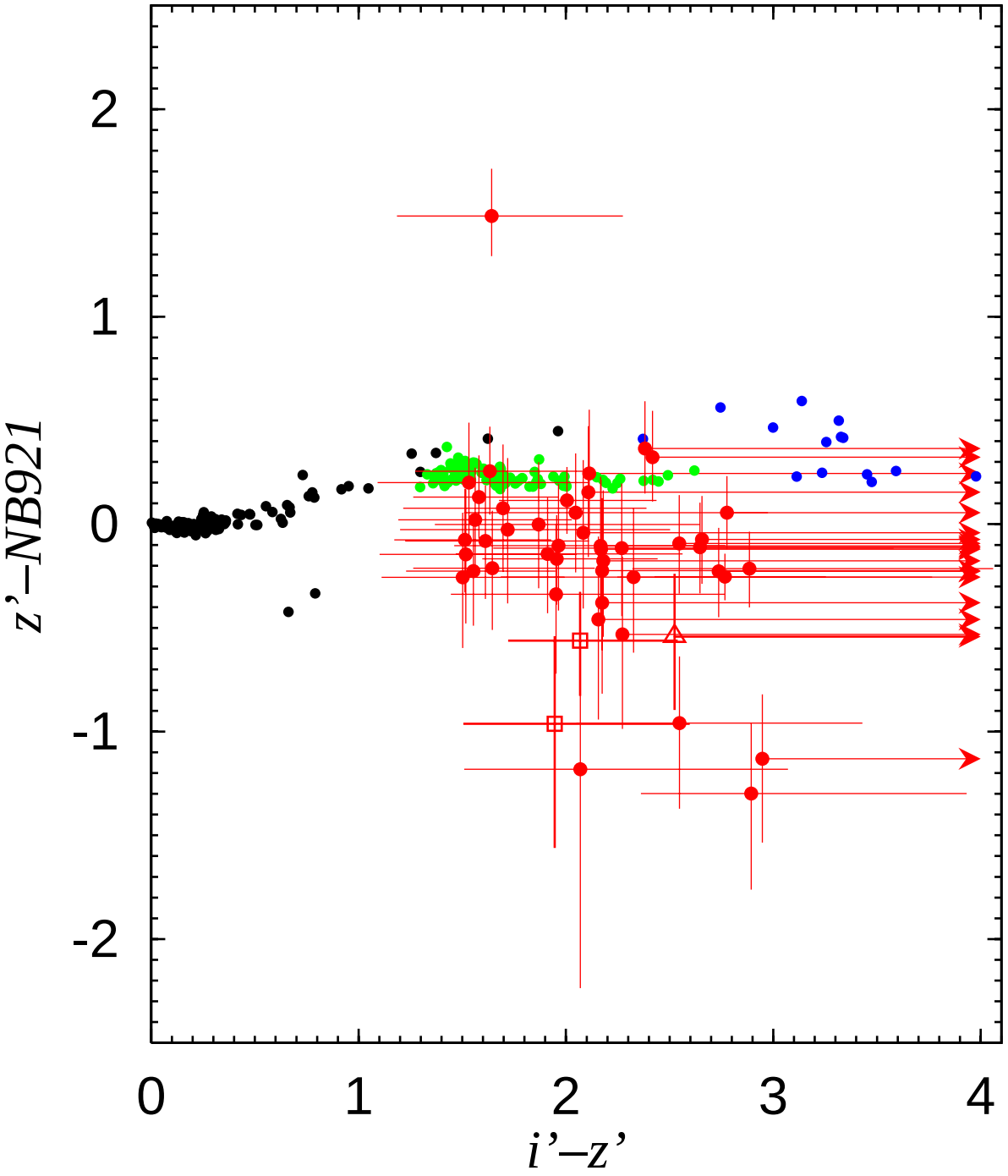

Fig. 4.— Photometric properties of Galactic stars and observed NB921-depressed i'-dropout objects plotted on $z' - NB921$ versus $i' - z'$ color-color diagram. Black, green, and blue filled circles denote Galactic M and earlier type stars (Gunn & Stryker 1983), L dwarfs and T dwarfs (Kirkpatrick 2003), respectively. The data of the NB921-depressed i'-dropout objects are shown by red points; among them, the two target objects (SDF J132426.5+271600 and SDF J132442.5+272423) are shown by open squares, and the object discussed by Nagao et al. (2004) is shown by a open triangle.

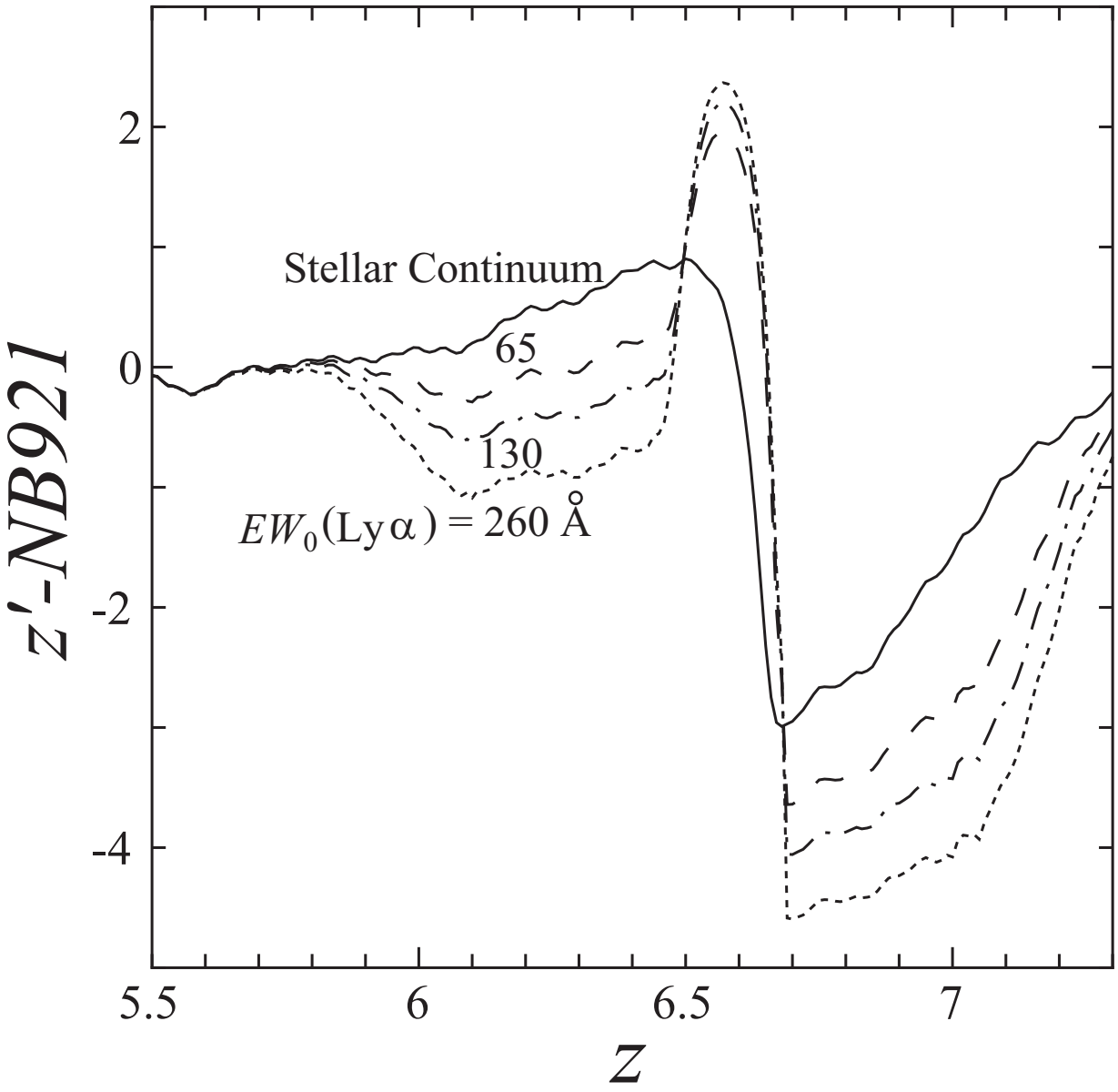

Fig. 5.— Expected $z' - NB921$ color predicted by the stellar population synthesis model, as a function of redshift. The solid, dashed, dash-dotted, and dotted lines denote the stellar SED with Lyα whose rest-frame equivalent width is 0, 65, 130, and 260 Å, respectively.

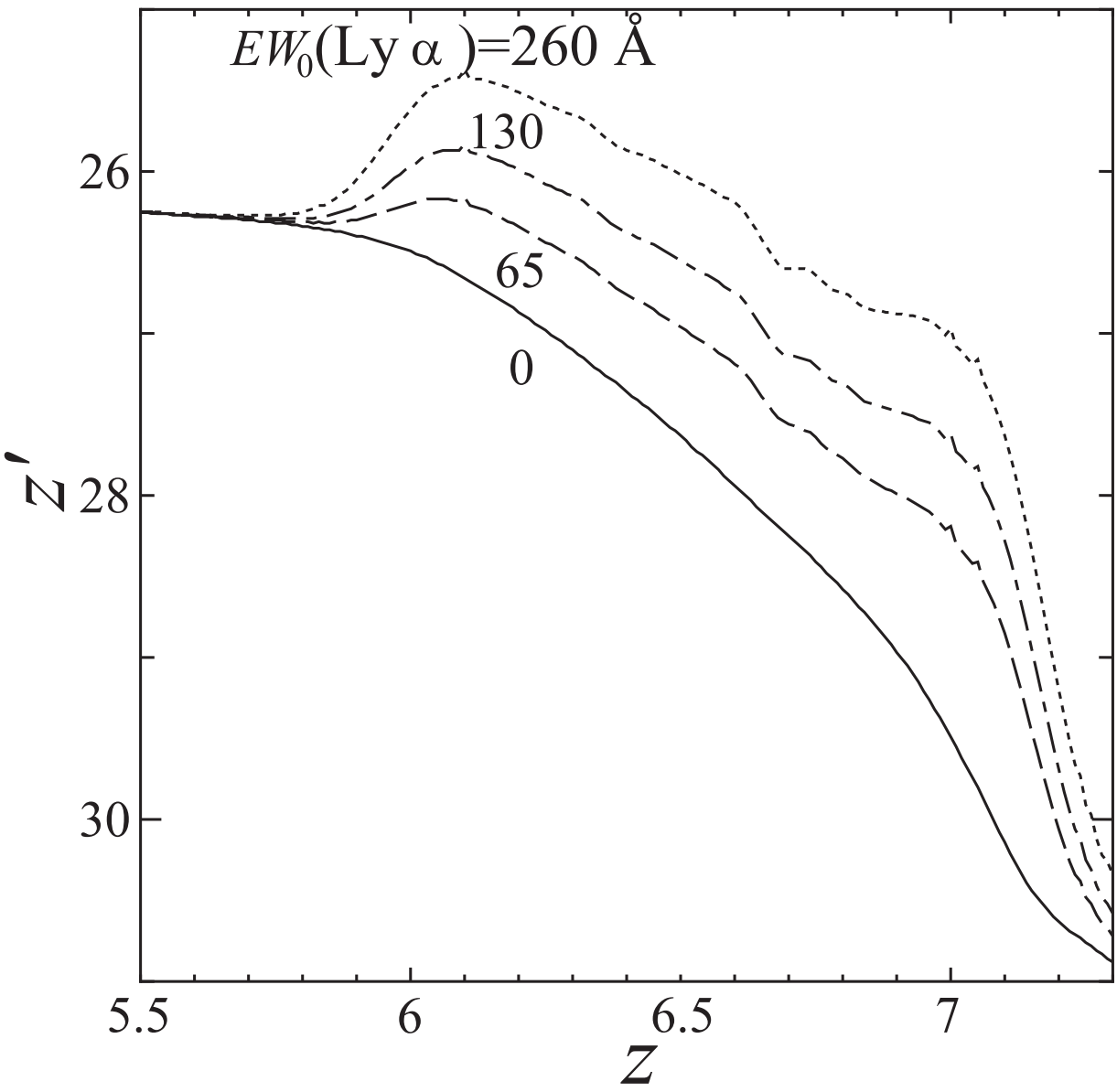

Fig. 6.— Expected z'-band magnitude of galaxies with $M_{1500} = -20.0$ as a function of redshift. The solid, dashed, dash-dotted, and dotted lines are the same as those in Figure 5.